On the activation and passivation of precursors for process-induced positive charges in Hf-dielectric stacks

M. H. Chang,[1] C. Z. Zhao,[1,a)] Z. Ji,[1] J. F. Zhang,[1,b)] G. Groeseneken,[2,c)] L. Pantisano,[2] S. De Gendt,[2,c)] and M. M. Heyns[2,b)]
[1]*School of Engineering, Liverpool John Moores University, Byrom Street, Liverpool L3 3AF, United Kingdom*
[2]*IMEC, Kapeldreef 75, B3001 Leuven, Belgium*

(Received 2 October 2008; accepted 29 January 2009; published online xx xx xxxx)

Hf-based dielectric stack is replacing SiON as gate dielectric even though our understanding of it is incomplete. It has been reported that a thermal exposure above 450 °C can lead to positive charging in both unoptimized SiO_2 layer and Hf-based dielectric stack. At present, there is little information on how this process-induced positive charging (PIPC) occurs in the Hf-based stack and how to suppress it. The objective of the current work is to improve our understanding by addressing three key issues. First, the activation of PIPC precursors after device fabrication is investigated and it will be shown that the loss of certain species from the gate edge through lateral diffusion is responsible for it. Second, the passivation of the precursor is studied and the relevant species are explored. It is found that both water- and chlorine-related species play a role. Finally, the reactivation of the passivated precursor is examined and the results show that it is not thermally accelerated. © *2009 American Institute of Physics*. [DOI: 10.1063/1.3093679]

I. INTRODUCTION

With the continuous downscaling of transistor size, Hf-based dielectric stack and metal gate are replacing the conventional SiON and polysilicon gate to satisfy gate leakage current requirement for complementary metal-oxide-semiconductor (CMOS) technologies. In comparison with a state-of-the-art SiON layer, Hf-based stacks have many problems, such as high defect density,[1–3] low carrier mobility,[4,5] process integration,[6,7] and reduced device lifetime.[8,9] To some extent, a Hf-based stack behaves like an unoptimized SiO_2 film.[10,11]

For an unoptimized SiO_2, it was reported that exposure to H_2 at a temperature of 450 °C or above could lead to substantial positive charging in the oxide.[12–16] This process-induced positive charging (PIPC) has been observed for both the buried oxide in a silicon-on-insulator structure[13,14] and gate SiO_2.[12,16] It is typically absent for a device-grade SiO_2. For high-*k* dielectrics, PIPC has been reported for both the Al-based[7] and Hf-based[17,18] dielectric layers. It is generally accepted that PIPC is hydrogen related.[12–18] Hydrogen can be supplied either externally from ambient gas or internally from the prestored hydrogenous species within the device. The latter is responsible for the PIPC when Hf stack was exposed to N_2.[17,18] PIPC has been observed in samples with different Hf concentrations, gate materials, and conduction channel polarities.[17,18]

Despite the early efforts, there are many questions remaining to be answered for the PIPC in Hf-based stacks. One of them is that PIPC can be absent in a device immediately after its fabrication, although it was annealed in forming gas at 520 °C. When the same device was annealed again at 500 °C after several months, substantial PIPC occurs. The precursor responsible for PIPC must be activated somehow during the storage and there is no information on it at present. Central to this work is to investigate the activation and passivation of PIPC precursors. It will be shown that certain species can diffuse out of the stack from the gate edge during storage, resulting in the activation. Adding H_2O- and Cl-related species to the sample passivates the precursor, and the passivation is insensitive to the device fabrication conditions. The passivation, however, is not permanent and the precursor can be reactivated. It is found that the reactivation is not a thermally accelerated process.

II. DEVICES AND EXPERIMENTS

A. Devices

Metal-oxide-semiconductor field effect transistors (MOSFETs) fabricated from four different batches were used in this work. Fabrication typically starts with an IMEC clean and a 0.4–1 nm chemical SiO_2.[19] This interfacial layer was nitrided in NH_3 at 900 °C for 60 s before depositing HfO_2. Both HfO_2 and Hf silicates were prepared by atomic layer deposition with an equivalent oxide thickness (EOT) in the range from 0.96 to 1.3 nm. The silicates have Hf concentration between 23% and 70% and were nitrided in NH_3 at 800 °C for 60 s. A 1000 °C spike was typically used to activate the source and drain, but there are also samples where the activation was by solid phase epitaxial regrowth (SPER) at 650 °C for 1 min. The gate material is either poly-Si or TaTiN, and the devices received a forming gas anneal at 520 °C for 20 min. The channel length and width are 0.14–10 μm and 10 μm, respectively. Details of the devices used for each test are given in figure legends or captions.

a)Present address: Xi'an Jiaotong-Liverpool University.
b)Electronic mail: j.f.zhang@ljmu.ac.uk.
c)Also at KU Leuven, Leuven, Belgium.

 © 2009 American Institute of Physics

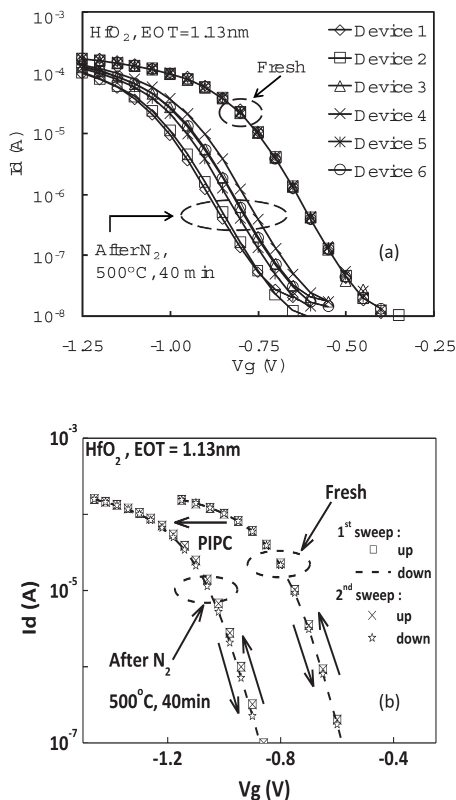

FIG. 1. PIPC in Hf-based dielectric stack. (a) shows that, in the fresh samples, there is little PIPC and the sample-to-sample variation is negligible. After a thermal exposure in N_2 at 500 °C for 40 min, the negative shift indicates PIPC formation that has a large sample-to-sample variation. (b) shows that the charge trapping induced hysteresis between the up- and down-traces of gate bias sweep is insignificant when compared with PIPC. The difference between the first and second V_g sweep is negligible. The *p*MOSFET has a TaTiN gate and was nitrided in NH_3 at 900 °C for 60 s before depositing a 2 nm HfO_2 layer.

B. Experiments

The test sequence starts with measuring the transfer characteristics (TCs) at a drain bias of 0.1 V. The device was then exposed to a typical temperature of 500–550 °C for 40–160 min in N_2. After the exposure, TC was measured again and the shift in TC, ΔV_{th}, was obtained by the standard extrapolation method.[20] Since PIPC generally has a considerable sample-to-sample variation,[16–18] the ΔV_{th} after thermal exposure was typically measured on 6–24 MOSFETs of the same sizes. When investigating the effect of channel length on PIPC, the average value, ΔV_{th_av}, was used to suppress the sample-to-sample variation.

III. RESULTS AND DISCUSSIONS

A. Activation and passivation of PIPC precursors

Figure 1(a) compares the transfer characteristics before and after thermal exposure at 500 °C. The negative shift indicates the PIPC in gate dielectric during the thermal exposure and the large sample-to-sample variation is a feature of PIPC.[16–18] Before this thermal exposure, the sample-to-sample variation is negligible and the measured threshold voltage agrees with its theoretical value, confirming insignificant PIPC in "fresh" samples. To show that the PIPC observed here is different from the stress-induced positive

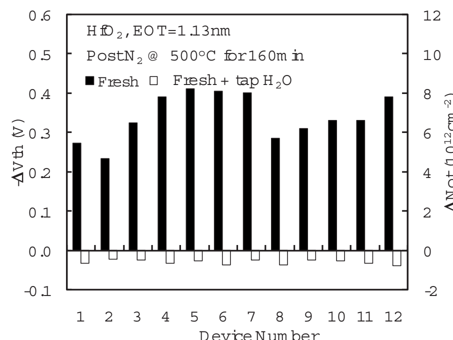

FIG. 2. Passivation of PIPC precursors. The solid bars represent results when samples were exposed to N_2 at 500 °C for 160 min. For the empty bars, the samples were first immersed in tap H_2O for 90 min at 100 °C and then subjected to the same thermal exposure at 500 °C for 160 min in N_2. The ΔN_{ot} is the effective charge density by assuming all charges at the dielectric/substrate interface. The device fabrication is the same as that in Fig. 1.

charge trapping,[10,11] Fig. 1(b) compares the PIPC and the trapping-induced hysteresis. It is clear that trapping is insignificant under our test conditions. Figure 1(b) also shows that there is little difference between the initial and a subsequent gate bias sweep.

A key question is why was the PIPC not formed when the fresh devices in Fig. 1 already received a standard 520 °C forming gas anneal at the end of the fabrication process. The device must be changed after the fabrication in some way. Our first thought is that the sample could be contaminated by water-related species, since they were stored in room air without capsulation for several months before the experiment in Fig. 1. To test it, an accelerated contamination experiment was designed to increase water contamination. In Fig. 2, two groups of devices were used: one was annealed directly in N_2 at 500 °C for 160 min (solid bars), while the other was first immersed in tap water for 90 min at 100 °C, to accelerate the contamination, before going through the same thermal exposure (empty bars). Against our expectation of an increase in PIPC, Fig. 2 shows that PIPC was actually suppressed after immersing devices in tap water.

To explain the above surprising phenomenon, we assume that the precursor for PIPC is *A*, although its microscopic structure is not known. During fabrication, some *A*–*X* bonds were formed in the dielectric and the precursor is inactive, so that PIPC is insignificant, as illustrated in Fig. 3(a). The *A*–*X*

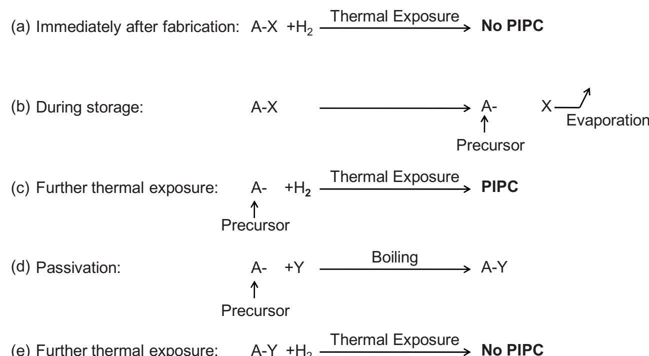

FIG. 3. A schematic illustration of the reactions for different stages in the formation and passivation of PIPC and its precursors.

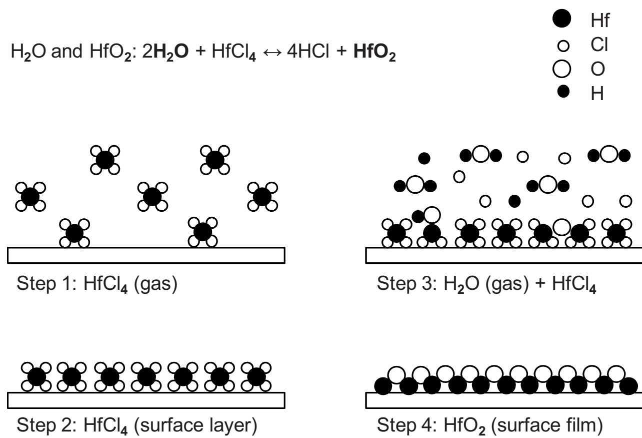

FIG. 4. A schematic illustration of the deposition process of Hf-dielectric layer. H_2O and $HfCl_4$ are the main ingredients in forming HfO_2.

132 bond may not be stable and could be broken during the stor-
133 age. Figure 3(b) shows that the *X* species could evaporate
134 and leave *A* behind. In this way, the precursor is activated
135 and reacts with H_2 to form PIPC during a subsequent thermal
136 exposure, as indicated in Fig. 3(c). When a sample is im-
137 mersed in tap water, some species *Y* may enter the device
138 and passivate the precursor by forming $A-Y$ bond, as illus-
139 trated in Fig. 3(d). Figure 3(e) illustrates why PIPC is negli-
140 gible after immersing the sample in tap water.

141 B. The *X* and *Y* species

142 In order to explore the species *X* and *Y*, we can look at
143 how the Hf dielectric layer was deposited. Figure 4 shows a
144 typical process flow,[21] where a surface layer was first depos-
AQ: #2 145 ited by $HfCl_4$ before the addition of H_2O to form HfO_2. As a
146 result, the species *X* and *Y* could be H_2O or Cl related. To
147 test whether H_2O alone is sufficient for passivating the pre-
148 cursor, we replaced tap water by de-ionized water. By using
149 the same test procedure as that in Fig. 2, Fig. 5(a) shows that
150 when the thermal exposure was 40 min, the passivation was
151 effective. However, if the thermal exposure was extended to
152 160 min, the passivation became ineffective, as shown in
153 Fig. 5(b). As a result, the passivation after immersing in de-
154 ionized water is less stable than that after immersing in tap
155 water, indicating H_2O alone is less effective.
156 Since chloride is one ingredient in Hf-dielectric fabrica-
157 tion, one may expect that Cl-related species are also involved
158 in the passivation. The tap water can contain some chloride
159 that was removed in the de-ionized water, resulting in the
160 difference between Figs. 2 and 5(b). To test this assumption,
161 in the experiment of Fig. 6, we added chloride to the de-
162 ionized water through NaCl. The empty bars in Fig. 6 show
163 that the passivation remains effective after the thermal expo-
164 sure was extended to 160 min, confirming the expectation.
165 This makes us believe that the species *X* and *Y* are related to
166 H_2O and Cl, although we do not know their detailed struc-
167 ture at present. It was reported that sodium can contaminate
168 the sample and cause additional positive charging.[22] The
169 PIPC passivation observed in Fig. 6 after exposing to NaCl,
170 however, shows that sodium does not introduce positive
171 charges under our test conditions.

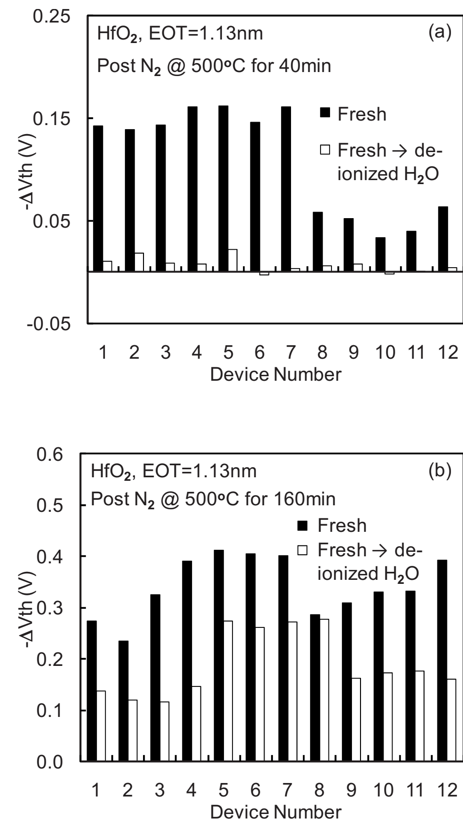

FIG. 5. Passivation by de-ionized water at 100 °C for 90 min. The thermal exposure was at 500 °C in N_2 for (a) 40 min and (b) 160 min. The empty and solid bars represent results with and without passivation, respectively. Although the passivation is effective at short time in (a), PIPC became substantial after an extended exposure in (b). The device fabrication is the same as that in Fig. 1.

C. Insensitivity of the passivation to fabrication conditions 172 173

The sample used up to now is $HfO_2/SiON$ with a TaTiN 174
gate and a spike activation at 1000 °C. Results show that 175
PIPC can also occur in Hf-silicates (Fig. 7), polysilicon gated 176
devices (Fig. 8), and samples activated by SPER at 650 °C 177
(Fig. 9). It is interesting to examine whether PIPC precursors 178
can also be effectively passivated in these samples. Figures 179
7–9 confirm that the passivation is equally effective, so that 180
the passivation is insensitive to the sample fabrication con- 181
ditions. 182

D. Out-diffusion path for the species *X* 183

As illustrated by Figs. 3(a)–3(c), the diffusion of species 184
X away from the dielectric activates the PIPC precursor, and 185
we investigate the diffusion path here. There are two possible 186
paths: one is vertical through the gate or substrate and the 187
other is lateral through the edge of the gate dielectric. If 188
species *X* diffused away vertically, one would expect that 189
PIPC is insensitive to channel length. Figure 10, however, 190
shows that PIPC decreases monotonously as channel length 191
increases, against the assumption of a vertical path. 192
Figure 11 illustrates that the channel length dependence 193
can be explained by a lateral diffusion through the edge. 194
Immediately after fabrication, *X* exists throughout the chan- 195
nel [Fig. 11(a)]. During storage, *X* near the edge will diffuse 196

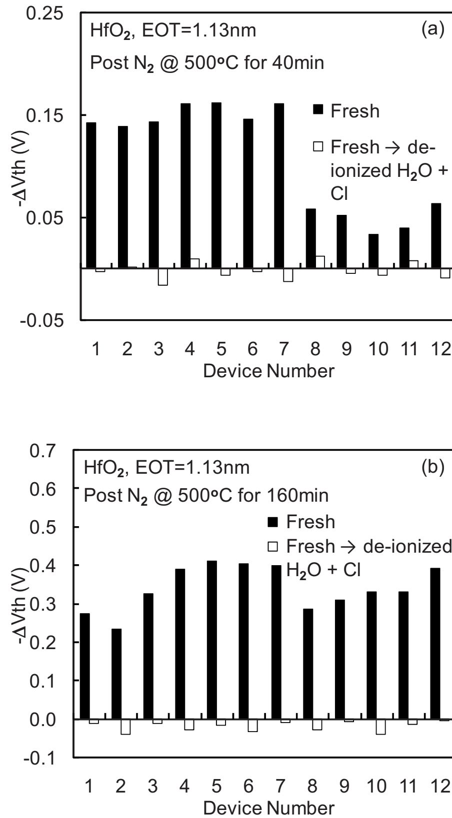

FIG. 6. Passivation by de-ionized water and chloride at 100 °C for 90 min. The thermal exposure was at 500 °C in N_2 for (a) 40 min and (b) 160 min. The empty and solid bars represent results with and without passivation, respectively. The passivation remains effective after 160 min exposure at 500 °C. The device fabrication is the same as that in Fig. 1.

away first and leave the activated precursors behind, as represented by the symbol "○" in Fig. 11(b). For a short channel device, a high percentage of the channel is activated. During the subsequent thermal exposure, the precursor becomes positively charged (symbol "●"), as shown in Fig. 11(c). It is clear that a short channel device has a high percentage of the channel with PIPC and this explains its larger ΔV_{th} in Fig. 10.

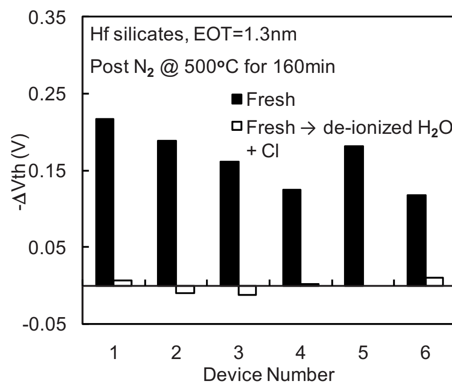

FIG. 7. Passivation by de-ionized water and chloride at 100 °C for 90 min. The thermal exposure was at 500 °C in N_2 for 160 min. The empty and solid bars represent results with and without passivation, respectively. The *p*MOSFET has a TaTiN gate. The Hf silicate is 1 nm with 70% Hf, nitrided in NH_3 at 800 °C for 60 s.

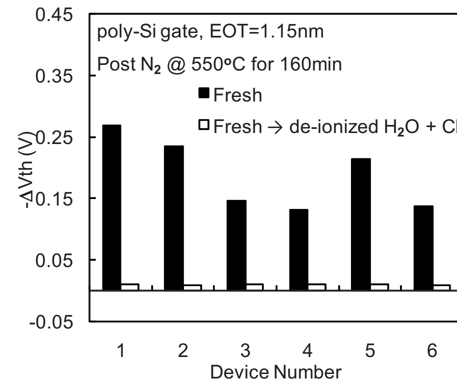

FIG. 8. Passivation by de-ionized water and chloride at 100 °C for 90 min. The thermal exposure was at 500 °C in N_2 for 160 min. The empty and solid bars represent results with and without passivation, respectively. The *n*MOSFET has a poly-Si gate and a 1.5 nm Hf silicate with 23% Hf, nitrided in NH_3 at 800 °C for 60 s.

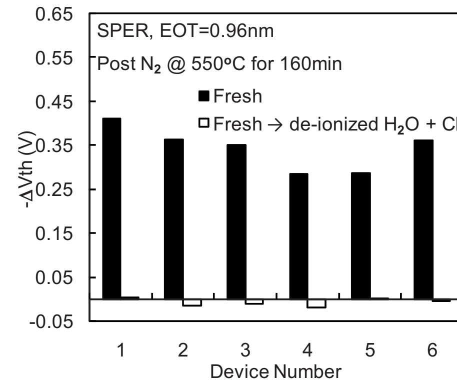

FIG. 9. Passivation by de-ionized water and chloride at 100 °C for 90 min. The thermal exposure was at 500 °C in N_2 for 160 min. The empty and solid bars represent results with and without passivation, respectively. The *n*MOSFETs have a 2 nm HfO_2 and a TaTiN gate. Unlike the other samples used in this work, the source and drain were activated by SPER at 650 °C for 60 s.

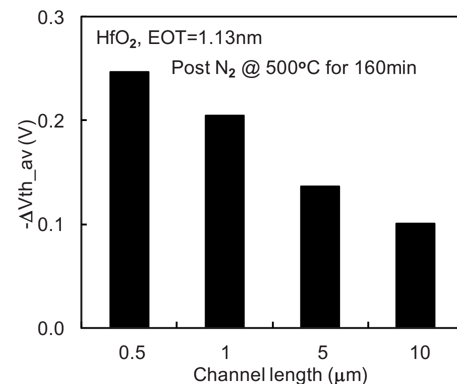

FIG. 10. Effects of channel length on PIPC formation. For each channel length, the averaged shift, ΔV_{th_av}, was obtained on 24 different samples. The thermal exposure was in N_2 at 500 °C for 160 min. The sample used is the same as that in Fig. 1.

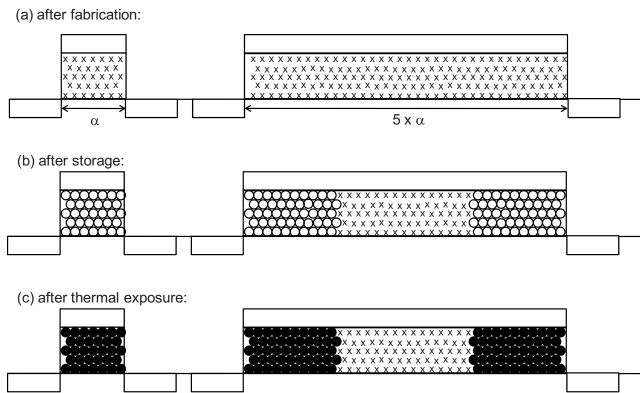

FIG. 11. A schematic illustration of the channel length dependence of the PIPC. (a) shows the case immediately after device fabrication. Symbol "×" represents a passivated PIPC precursor. The symbol "○" in (b) represents an activated PIPC precursor after × diffused out through the gate edge. The symbol "●" in (c) represents PIPC after a thermal exposure.

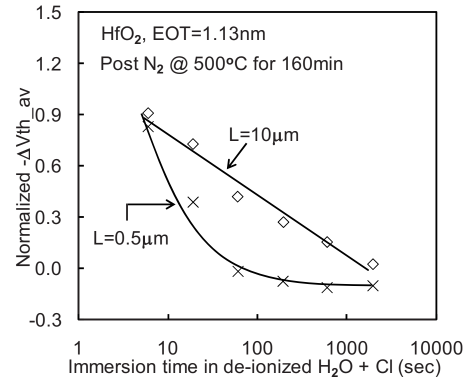

FIG. 13. Passivation kinetics for long ($L=10$ μm, symbol "◇") and short ($L=0.5$ μm, symbol "×") channel devices. For a given passivation time, the averaged shift, ΔV_{th_av}, was normalized against the one without passivation. Lines serve as a guide for the eye. The sample used is the same as that in Fig. 1.

205 ## E. In-diffusion path for the species *Y*

206 After examining the out-diffusion path of *X* for precursor
207 activation, we now study the in-diffusion path of species *Y*
208 for precursor passivation. *Y* can diffuse into the device either
209 vertically or laterally, and we again use the channel length
210 dependence to determine the path.

211 In Figs. 6–9, samples were immersed in H_2O and Cl
212 solution for 90 min and full passivation was observed for
213 both short and long channel devices. This can be achieved by
214 in-diffusion either vertically or laterally, so that conclusion
215 cannot be drawn. To determine the path, the immersion time
216 must be reduced to a level such that full passivation is not
217 reached for all devices. Figure 12 shows that an immersion
218 time of 6 s is too short for the in-diffusion. When increased
219 to 60 s, the passivation is completed for the shortest channel
220 ($L=0.5$ μm), but the normalized ΔV_{th} now increases with
221 channel length. Figure 13 gives a more detailed dependence
222 of passivation on the immersion time, and the shorter device
223 clearly needs less time. This channel length dependence sup-
224 ports the lateral in-diffusion of *Y*. As illustrated in Figs.
225 14(a)–14(c), for a given immersion time such as 60 s, the
226 passivation is completed for the short channel but not for the
227 long channel.

228 ## F. Reactivation after passivation

229 We propose that the out-diffusion of species *X* during
230 storage activated the precursor and that in-diffusion of spe-
231 cies *Y* passivated it. One may ask whether *X* and *Y* are the
232 same species and if the passivated precursor $A-Y$ can also be
233 reactivated like the original $A-X$. In Fig. 15, two groups of
234 samples were passivated. One of them was exposed at
235 500 °C immediately after passivation, while the other was
236 stored in room temperature for 30 days before receiving the
237 same thermal exposure. As expected, PIPC was negligible
238 for the devices immediately exposed after passivation
239 (stripped bars). However, significant PIPC occurred after a
240 storage of 30 days (solid bars). This indicates that, like the
241 original species *X*, the species *Y* can also diffuse out during
242 storage. Despite their similar properties, the lack of knowl-
243 edge on their microscopic structure does not allow us to
244 draw a definitive conclusion on whether these two are iden-
245 tical.

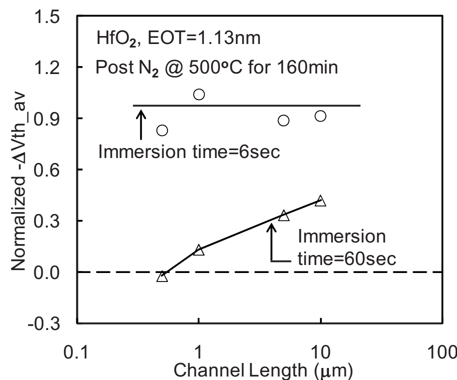

FIG. 12. Effects of channel length on PIPC precursor passivation. Three groups of devices were used. One group was not passivated. The other two went through the passivation step in de-ionized water and chloride at 100 °C with passivation times of 6 and 60 s, respectively. For each channel length, the averaged shift, ΔV_{th_av}, was normalized against the one without passivation. The thermal exposure was in N_2 at 500 °C for 160 min for all three groups. The sample used is the same as that in Fig. 1.

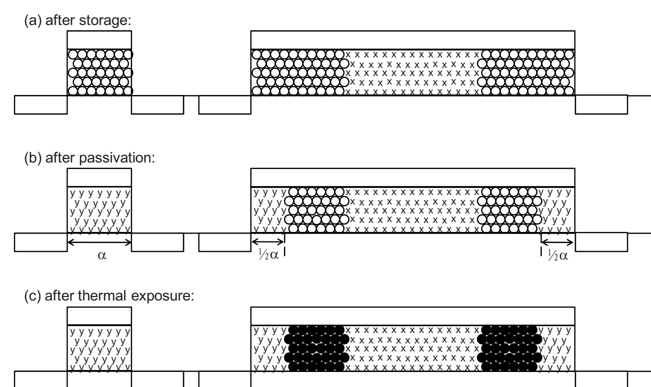

FIG. 14. A schematic illustration of the channel length dependence of the precursor passivation. (a) shows the case after the precursor is activated during the storage. The symbols "○" and "×" represent an activated and passivated precursor, respectively. The symbol "y" in (b) represents a repassivated precursor. The symbol "●" in (c) represents positive charges after a thermal exposure.

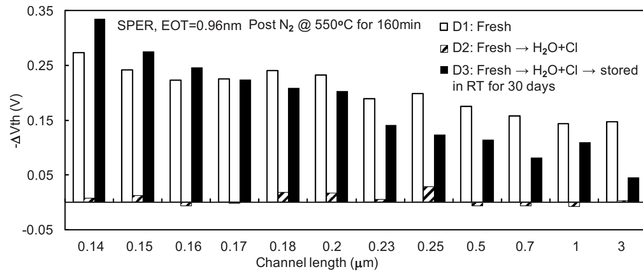

FIG. 15. Reactivation of PIPC precursors after passivation. Three groups of devices were used. One of them (D1, empty bars) was not passivated, but the other two were passivated in de-ionized water and chloride at 100 °C for 90 min. After the passivation, one group (D2, stripped bars) was immediately exposed to N_2 at 550 °C for 160 min. After storage at room temperature in air for 30 days, the last group (D3, solid bars) was also exposed to N_2 at 550 °C for 160 min.

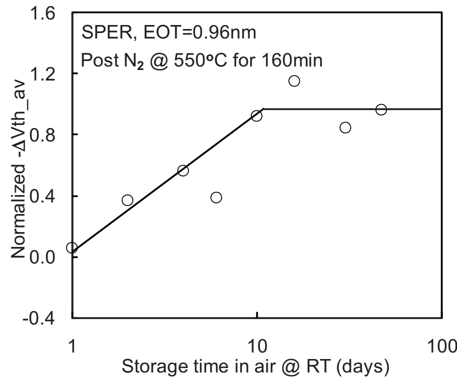

FIG. 16. Effects of storage time on the precursor reactivation. Eight groups of devices were passivated and then stored at room temperature for 1, 2, 4, 6, 10, 16, 30, and 47 days, respectively. After the storage, all samples were exposed to N_2 at 550 °C for 160 min. Lines serve as a guide to the eye. The samples used are the same as that in Fig. 9.

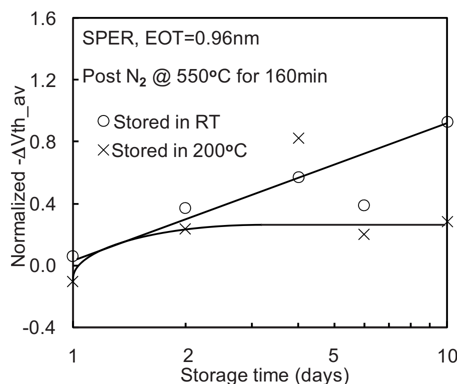

FIG. 17. Effects of storage temperature on the precursor reactivation. Ten groups of devices were passivated. Half of them were then stored in room temperature, and the other half stored in 200 °C for 1, 2, 4, 6, and 10 days, respectively. After the storage, all samples were exposed to N_2 at 550 °C for 160 min. Lines serve as a guide to the eye. The samples used are the same as that in Fig. 9.

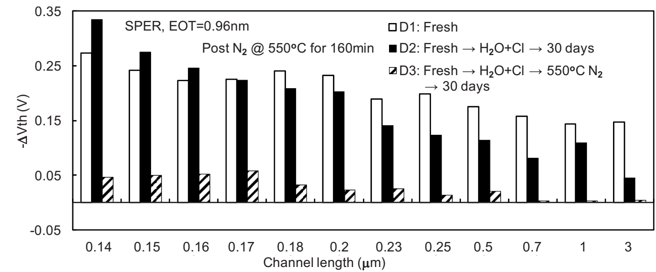

FIG. 18. Effects of thermal energy on the passivated precursor bonds. Three groups of devices were used. One of them (D1, empty bars) was not passivated, but the other two were passivated in de-ionized water and chloride at 100 °C for 90 min. After the passivation, one group (D3, stripped bars) was immediately exposed to N_2 at 550 °C for 160 min, while the other (D2, solid bars) was not. Both groups were then stored at room temperature and air for 30 days before they were exposed to N_2 at 550 °C for 160 min. The sample used is the same as that in Fig. 9.

To characterize the out-diffusion kinetics of species Y, the same experiment as in Fig. 15 was carried out with another seven groups of devices with storage times of 1, 2, 4, 6, 10, 16, and 47 days, respectively. Figure 16 shows that a full dissociation was reached in about 10 days.

We now explore the effects of storage temperature on precursor reactivation. Passivated devices were stored at either room temperature (RT) or 200 °C for 1, 2, 4, 6, and 10 days. Figure 17 shows that, within our experimental resolution, the reactivation is not thermally accelerated. To further explore this issue, one group of devices was exposed at 550 °C immediately after the passivation step. The devices were then stored in RT for 30 days before a second 550 °C exposure. Figure 18 shows that the PIPC became substantially smaller. This suggests that $A-Y$ bonds became more stable after the prestorage 550 °C exposure, so that their dissociation during the storage was slowed down.

IV. CONCLUSION

This work investigates the activation and passivation of precursors for the PIPC in a Hf-based dielectric stack. Although the precursor is inactive and PIPC is not formed during the device fabrication, some species X can diffuse out the dielectric stack during the storage, leading to the activation of PIPC precursors. The precursor can be passivated by the species Y after immersing the sample in H_2O and chloride solution. This passivation is insensitive to the device fabrication conditions.

The diffusion path of species X and Y is explored by investigating its channel length dependence. The results show that the species X diffuses laterally through the edge of the gate dielectric, rather than vertically through the gate, during the storage. During passivation, the species Y also enters the gate dielectric laterally through the edge. Although the lack of knowledge on the microscopic structure of X and Y does not allow us to conclude that they are the same, we found that they have similar properties. Like X, Y can also be lost during storage, resulting in the reactivation of the precursor. The reactivation is not thermally accelerated, and results indicate that the passivation bonding becomes more stable at higher temperature.

286 ## ACKNOWLEDGMENTS

287 This work is supported by the Engineering and Physical 288 Sciences Research Council of UK under Grant No. EP/ 289 C003071/1.

290 [1]T. P. Ma, H. M. Bu, X. W. Wang, L. Y. Song, W. He, M. Wang, H.-H. 291 Tseng, and P. J. Tobin, IEEE Trans. Device Mater. Reliab. **5**, 36 (2005).
292 [2]C. Z. Zhao, J. F. Zhang, M. B. Zahid, B. Govoreanu, G. Groeseneken, and 293 S. De Gendt, J. Appl. Phys. **100**, 093716 (2006).
294 [3]P. K. Hurley, K. Cherkaoui, E. O'connor, M. C. Lemme, H. D. B. Gottlob, 295 M. Schmidt, S. Hall, Y. Lu, O. Buiu, B. Raeissi, J. Piscator, O. Engstrom, 296 and S. B. Newcomb, J. Electrochem. Soc. **155**, G13 (2008).
297 [4]W. J. Zhu and T. P. Ma, IEEE Electron Device Lett. **25**, 89 (2004).
298 [5]M. Fischetti, D. Neumayer, and E. Cartier, J. Appl. Phys. **90**, 4587 (2001).
299 [6]S. Stemmer, Y. L. Li, B. Foran, P. S. Lysaght, S. K. Streiffer, P. Fuoss, and 300 S. Seifert, Appl. Phys. Lett. **83**, 3141 (2003).
301 [7]J. Westlinder, T. Schram, L. Pantisano, E. Cartier, A. Kerber, G. S. Lujan, 302 J. Olsson, and G. Groeseneken, IEEE Electron Device Lett. **24**, 550 303 (2003).
304 [8]M. Houssa, M. Aoulaiche, S. Van Elshocht, S. De Gendt, G. Groeseneken, 305 and M. Heyns, Appl. Phys. Lett. **86**, 173 (2005).
306 [9]Z. M. Rittersma, J. J. G. P. Loo, Y. V. Ponomarev, M. A. Verheijen, M. 307 Kaiser, F. Roozeboom, S. Van Elshocht, and M. Caymax, J. Electrochem. 308 Soc. **151**, G870 (2004).
309 [10]J. F. Zhang, C. Z. Zhao, M. H. Chang, M. B. Zahid, A. R. Peaker, S. Hall, G. Groeseneken, L. Pantisano, S. De Gendt, and M. Heyns, Appl. Phys. 310 Lett. **92**, 013502 (2008). 311
[11]C. Z. Zhao, J. F. Zhang, M. H. Chang, A. R. Peaker, S. Hall, G. Groe- 312 seneken, L. Pantisano, S. De Gendt, and M. Heyns, IEEE Trans. Electron 313 Devices **55**, 1647 (2008). 314
[12]K. Vanheusden, W. L. Warren, R. A. B. Devine, D. M. Fleetwood, J. R. 315 Schwank, M. R. Shaneyfelt, P. S. Winokur, and Z. J. Lemnios, Nature 316 (London) **386**, 587 (1997). 317
[13]R. E. Stahlbush, R. K. Lawrence, and H. L. Hughes, IEEE Trans. Nucl. 318 Sci. **45**, 2398 (1998). 319
[14]P. J. Macfarlane and R. E. Stahlbush, Appl. Phys. Lett. **77**, 3081 (2000). 320
[15]J. F. Zhang, C. Z. Zhao, G. Groeseneken, R. Degraeve, J. N. Ellis, and C. 321 D. Beech, Solid-State Electron. **46**, 1839 (2002). 322
[16]J. F. Zhang, C. Z. Zhao, G. Groeseneken, R. Degraeve, J. N. Ellis, and C. 323 D. Beech, J. Appl. Phys. **90**, 1911 (2001). 324
[17]C. Z. Zhao, J. F. Zhang, M. B. Zahid, E. Efthymiou, Y. Lu, S. Hall, A. R. 325 Peaker, G. Groeseneken, L. Pantisano, R. Degraeve, S. De Gendt, and M. 326 Heyns, Microelectron. Eng. **84**, 2354 (2007). 327
[18]C. Z. Zhao, J. F. Zhang, M. H. Chang, A. R. Peaker, S. Hall, G. Groe- 328 seneken, L. Pantisano, S. De Gendt, and M. Heyns, J. Appl. Phys. **103**, 329 014507 (2008). 330
[19]F. De Smedt, C. Vinckier, I. Cornelissen, S. De Gendt, and M. Heyns, J. 331 Electrochem. Soc. **147**, 1124 (2000). 332
[20]M. H. Chang and J. F. Zhang, J. Appl. Phys. **101**, 024516 (2007). 333
[21]D. J. DiMaria, J. Appl. Phys. **52**, 7251 (1981). 334
[22]Y. Widjaja and C. B. Musgrave, J. Chem. Phys. **117**, 1931 (2002). 335

AUTHOR QUERIES — 024906JAP

#1 Au: Please check our changes in ″A key question...″
#2 Au: References must be cited in order. Please check our renumbering of Refs. 21 and 22.